Air-mass trajectories and extreme episodes: snowfalls on the south-east coast of the Iberian Peninsula between 1900 and 2005.

Emilio Martínez-Ibarra[a], Francisco Javier Bello-Millán[b, c], Juan Garrido-Clavero[a]

a Universidad de Granada, Granada (España)

b AEMET (State Meteorological Agency), Malaga, Spain

c Universidad de Málaga, Málaga (España)

Corresponding author: Emilio Martínez-Ibarra, emibarra@ugr.es

Abstract: This paper analyses and characterizes snowfall events in one of the hottest, most arid areas in continental Europe. Our information was taken from a snowfall database that was partly our own, covering a period of over 100 years. The FLEXTRA model of air-mass back-trajectories was applied together with our own subjective synoptic classification. Data from the ECMWF Reanalysis of the 20th Century (ERA-20C) were used for the calculation and clustering of the back-trajectories and the establishment of synoptic weather types. The snowfall events were classified into 8 synoptic types and 4 first-level and 8 second-level back-trajectories. The meteorological scenario for these extreme events was marked by mixed structures at altitude with a main NE/SW axis and dipoles on the surface dominated by powerful North Atlantic anti-cyclones and back-trajectories from the NE at the three levels analysed (500, 1500 and 5000 m.a.s.l.).

Keywords: extreme meteorological events; snowfalls; SE coast of the Iberian Peninsula; back-trajectories; FLEXTRA model; subjective synoptic patterns.

1. Introduction

The weather in Europe is marked by abnormally hot and cold periods (Falarz, 2007) that can last for several consecutive days or sometimes even weeks (Bednorz, 2013). During the cold spells, there may be strong snowfalls (Frei and Robinson, 1999). Despite this, little research has been done on snow in Europe. Studies on this question tend to focus on: 1) the Alps (Satyawali et al., 2009; Valt et al., 2008; Soncini and Bocchiola, 2011; Scherrer et al., 2013); 2) areas with cold winters in Central Europe (Bednorz, 2004; Falarz, M., 2007; Bulygina et al., 2009; Bednorz, 2013; Szwed et al., 2017); and 3) Northern Europe (Bednorz, 2004; Bulygina et al., 2009; Bednorz, 2013). Analyses covering Europe as a whole (Henderson and Leathers, 2010; Croce P et al., 2021) or its Mediterranean area (Núñez-Mora et al., 2016) are much rarer and there are very few studies of mountain (Dafis S et al., 2016) or coastal regions of the Mediterranean (Houssos et al. 2007).

In Spain, snow has generally been considered a minor risk (Calvo, 2000). Research on this question has been far from prolific (Martínez-Ibarra, et al., 2019) and has focused above all on northern Spain (e.g. Ruíz, 1998; Pons et al., 2010; Merino et al., 2014; Núñez-Mora et al., 2016; de Pablo F et al., 2021) and mountainous areas (e.g. Herrero *et al.,* 2009; Buisan et al., 2015; Buisan et al., 2016; Pérez-Palazón et al., 2018). On rare occasions, papers about the Mediterranean region have been published (e.g. Salamanca-Salamanca 2012; Núñez-Mora et al., 2016), concentrating on either its inland (e.g. Olcina

& Moltó, 1999; Moltó, 2000) or coastal areas (e.g. Tomás-Quevedo, 1976; Martínez-Ibarra, et al. 2019). Snowfalls only affect the Mediterranean coast itself during extreme weather events. Research into such events includes studies of the SE of the Iberian Peninsula (Martínez-Ibarra, 2019), the city of Barcelona (Tomás-Quevedo, 1976), the coast of the island of Mallorca (Salamanca-Salamanca 2012), southeast France (Dauphiné, 1972), the coast of the Italian peninsula (Enzi et al., 2014) or the Greek capital, Athens (Houssos et al. 2007).

One of the best ways of understanding meteorological episodes of this kind is by studying air-mass trajectories (García, et al., 2005; Bednorz, 2013; Pérez et al., 2015). With this in mind, in this paper we will be studying snowfalls on the coast of SE Iberia by analysing the back-trajectories of the air masses involved.

Air-mass trajectories are often investigated using satellite images and more often mathematical models, which are versatile and easy to apply (Pérez et al., 2015). The most commonly used models include: 1) HYSPLIT (Hybrid Single-Particle Lagrangian Integrated Trajectories), described in Draxler (1992) and Draxler et al. (2003); 2) The FLEXTRA model, described by Stohl et al. (1995) and Stohl (1999); and the more recent METEX (Meteorological Data Explorer) model, described by Zeng et al. (2010). These models are used to identify trajectory sectors (Li et al., 2012) and conduct cluster analyses on the basis of various different techniques (Kassomenos et al., 2010).

The study of air-mass trajectories has proved particularly useful in the analysis of aerosols (Osada et al., 2003; Wilson et al., 2011; Esteve et al., 2012 Korgo et al., 2013) and atmospheric pollution (Osada et al., 2003; Levy et al., 2008; Seagram et al., 2013; Walna et al., 2013; Hernández-Ceballos and De Felice, 2019), especially in the study of long-range transport (Asaf et al., 2008; Kaiser, 2009; Datta et al., 2010; Hien et l., 2011; MacDonald et al., 2011; Westgate et al., 2013). Within meteorology, work tends to centre on its synoptic branch and the study of extreme events such as: 1) deep cyclogenesis (Innes et al., 2009); 2) MEDICANES (Fita et al., 2009); 3) episodes of intense rainfall (Tosic and M. Unkasevic, 2013; Trapero et al., 2013); 4) severe storms (Banacos and Ekster, 2010) with intense hailstorms (Banacos and Ekster, 2010) and tornados (Banacos and Ekster, 2010; Knox et al., 2013). It is also related with temperature analysis (Harpaz et al., 2014), cold advections (Soltani et al., 2014) and the study of generalized frost (Müller and Ambrizzi, 2010). Other issues that researchers have worked on include: 1) major forest fires (Pollina et al., 2013); 2) land-atmosphere moisture exchanges (Roberge et al., 2009; Knippertz and H.Wernli, 2010; Chubb et al., 2011; Drumond et al., 2011; Pfahl & Niedermann; 2011; Chen et al., 2012; Hernández-Ceballos et al., Hernández-Ceballos et al., 2013; Knippertz et al., 2013) and 3) cloud cover (Feingold et al., 2003; Mauger and Norris, 2010; Shi et al., 2010; Engel et al., 2013).
In recent years, in Spain there has been something of a proliferation of air-mass back-trajectory studies (**Table 1**). The questions explored in these papers centre above all on atmospheric pollution, especially of CO_2 and CH_4 (Pérez et al., 2018a; Pérez et al., 2018b; Pérez et al., 2019; Fernández-Duque et al., 2020) and O_3 (San José, et al., 2005; García et al., 2005; Adame et al., 2012a; Saavedra et al., 2012; Notario et al., 2014; Domínguez-López, et al., 2015). They have also analysed other pollutants such as NO_2 (Adame et al., 2012a; Adame et al., 2012b; Notario et al., 2014), SO_2 (Adame et al., 2012b; Notario et al., 2014), CO (Adame et al., 2012b), PM_{10} (Escudero et al., 2006; Stein et al, 2011;

Adame et al., 2012b; Notario et al., 2014) and even the radioactivity associated with aerosols (Dueñas et al., 2011; Valenzuela et al., 2012).

In the Iberian Peninsula, other more strictly meteorological issues have been analysed as either the main theme or as a complementary part of the study. We could cite for example: 1) cluster analysis of trajectories (Jorba et al., 2004; Pérez et al., 2015); 2) analysis of synoptic patterns (Saavedra et al., 2012); 3) the study of dust intrusions (Escudero et al., 2006; Stein et al, 2011; Valenzuela et al., 2012; 4) aerosol turbidity (Obregón et al., 2012); 5) precipitations (Izquierdo, Alarcón & Ávila, 2013); or 6), heatwaves (Hernández-Ceballos, Brattich & Cinelli, 2016). Studies have also been conducted into the aerosols produced by volcanic eruptions (Revuelta et al., 2012) forest fires (Ortiz-Amezcua et al., 2014), air masses as a vector for viral disease (García-Lastra et al., 2012) or olive pollen (Hernandez-Ceballos, et al., 2014; Fernández-Rodríguez et al., 2014).

Table 1. Studies of air-mass back-trajectories for the Iberian Peninsula

Subject/area of study	Back-trajectory technique, trajectory length and atmospheric levels studied	Trajectory analysis	Complementary analyses applied	Source
Air-mass trajectories /NE Iberian Peninsula (one observatory, Barcelona city)	HYSPLIT model, 96-h at 1500, 3000 and 5000 m.a.s.l.	Objective back-trajectory clusters (clusters-mean trajectories based on speed and direction of the trajectory)		Jorba et al. (2004)
Atmospheric pollution (Tropospheric ozone)/ northern plateau of the Iberian Peninsula (one observatory: Low Atmosphere Research Centre, CIBA)	HYSPLIT model, 72-h 1500 m.a.s.l (850 hPa)	Subjective back-trajectory clusters	Subjective 500-hPa synoptic weather patterns	García et al. (2005)
Atmospheric pollution (surface ozone)/ southern plateau of the Iberian Peninsula (various observatories Madrid city)	FLEXTRA model, 168-h		Atmospheric soundings Surface synoptic weather charts	San José et al. (2005)
Aerosols (dust from North Africa, concentrations from PM10)/ southern plateau of the Iberian Peninsula (one observatory, Risco Llano, Toledo province)	HYSPLIT model, 120-h at 500, 1500, and 2500 m.a.g.l.	Vertical profile	HYSPLIT dust concentration maps 850-hPa synoptic weather charts	Escudero et al (2006)
Aerosols (dust from North Africa, from PM10) / Andalusia	HYSPLIT model, 120-h at 500, 1500, and 2500 m.a.s.l.		HYSPLIT dust concentration maps Satellite images	Stein et al. (2011)

Aerosols (radionuclide activities :7Be and 210Pb)/ South Iberian Peninsula (one observatory, Malaga city)	HYSPLIT model, 96-h at 500, 1500 and 3000 m.a.s.l.	Objective back-trajectory clusters (origin and displacement velocity)	Synoptic patterns (700, 850 and 1000 hPa geopotential height for the days assigned to each of the identified clusters)	Dueñas et al. (2011)
Atmospheric pollution (NO2 and SO2)/ southern plateau of the Iberian Peninsula (one observatory, DOAS System, Puertollano, Ciudad Real province)	HYSPLIT model, 48-h, at 100 m.a.g.l.	Vertical profile		Adame et al. (2012a)
Atmospheric pollution (as a result of "medium"-range transport of air masses from wildfires: surface ozone, NO2, CO and PM10)/ southwestern Iberian Peninsula (western Andalusia)	HYSPLIT model, 72-h at 500 m.a.g.l.	Vertical profile	Satellite images, synoptic chart at surface (pressure) and 850 hPa (geopotential and temperature) Wind and specific humidity fields obtained using the WRF model in the finer domain	Adame et al. (2012b)
Virus/ Northern Iberian Peninsula (Basque Country)	HYSPLIT model, 72-h t 10, 500 and 1000 m a.g.l.	Vertical profile	Winds at surface	García-Lastra et al. (2012)
Aerosols (based on columnar properties of aerosols)/ Southwest Iberian Peninsula	HYSPLIT model, 120-h at 500, 1500 and 3000 m.a.g.l.	Subjective back-trajectory clusters (according to trajectory route: maritime and overland)		Obregón et al. (2012)
Atmospheric pollution (CO_2)/ northern plateau of the Iberian Peninsula (one observatory: Low Atmosphere Research Centre, CIBA)	Nonparametric Trajectory analysis, 9.5-h,	Objective back-trajectory clusters (average linkage method (Cape et al., 2000)		Pérez et al. (2012)
Aerosols (volcanic plume) / southern plateau of the Iberian Peninsula (CIEMAT site, Madrid city)	FLEXTRA model, 168-h at 1500, 3000 and 5000 m.a.g.l.		Lidar remote sensing	Revuelta et al. (2012)
Atmospheric pollution (surface ozone)/ northwestern Iberia (Galicia)	HYSPLIT model, 72-h at 500 and 1500 m a.g.l.	Subjective back-trajectory clusters (according to trajectory route: a) Mediterranean–Peninsular, b) and c) South Atlantic–Portuguese, d) regional/internal,	Synoptic patterns using a subjective classification (developed for the Iberian Peninsula by Font-Tullot, 1983)	Saavedra et al. (2012)

		e) French–Cantabrian, and f) British.) Vertical profile	850-hPa synoptic weather charts	
Aerosols (dust from North Africa, based on aerosol radiative properties)/southeastern Spain (Granada city)	HYSPLIT model, 120-h at 500, 1500, and 3000 m.a.g.l.	Objective back-trajectory clusters (clusters-mean trajectories based on speed and direction of the trajectory) Vertical profile	850-hPa synoptic weather charts (Subjective weather patterns= charts main synoptic scenarios) Satellite images	Valenzuela et al. (2012)
Chemical composition of precipitation /NE Iberian Peninsula (one observatory from Catalan Pre-coastal Range)	HYSPLIT model, 96-h at 1500 m.a.s.l.	Objective back-trajectory clusters (implemented in the HYSPLIT model)	WeMO index (WeMOi)	Izquierdo, Alarcón and Ávila (2013)
Chemical composition of precipitation (dissolved organic matter)/ Southwest Iberian Peninsula (only one observatory, Aveiro, Portugal)	HYSPLIT model, 48-h at 10 and 500 m.a.s.l.	Vertical profile		Santos et al. (2013)
Aerosols (olive pollen)/ Southwest Iberian Peninsula	HYSPLIT model, 48-h at 200 and 500 m.a.s.l.		Raster image about fraction olive grove coverage	Fernández-Rodríguez et al. (2014)
Aerosols (olive pollen)/ South Iberian Peninsula (one observatory, Cordoba city)	HYSPLIT model, 28-h at 100, 300, 500, 700 and 1000 m.a.g.l.	Vertical profile	Synoptic chart at surface (pressure)	Hernández-Ceballos et al. (2014)
Atmospheric pollution (NO, NO 2, O 3, SO 2 and PM10)/ southern plateau of the Iberian Peninsula	HYSPLIT model, 48-h, at 100 m.a.g.l.	Objective back-trajectory clusters (implemented in the HYSPLIT model)		Notario et al. (2014)
Aerosols (particles from forest fires)/southeastern Spain (Granada city)	HYSPLIT model, 240-h at 1000, 2000, 3000, 4000, 5000 and 6000 m.a.s.l.	Vertical profile	Lidar remote sensing	Ortiz-Amezcua et al. (2014)
Atmospheric pollution (Tropospheric ozone)/ Southwest Iberian Peninsula (western Andalusia)	HYSPLIT model, 72-h at 500 m.a.g.l.		Surface synoptic weather charts	Domínguez-López (2015)
Air-mass trajectories/ northern plateau of the Iberian Peninsula (one observatory: Low	METEX model, 48-h	Objective back-trajectory clusters (directions and distances covered)		Pérez et al. (2015)

Atmosphere Research Centre, CIBA)				
Heat waves and aerosols (radionuclide activities, 7Be concentrations)/Spain (cities of Seville, Madrid and Bilbao)	HYSPLIT model, 120-h, at 500, 1500, and 3000 m.a.g.l.	Objective back-trajectory clusters (implemented in the HYSPLIT model) Vertical profile		Hernández-Ceballos, Brattich and Cinelli (2016)
Atmospheric pollution (CO_2 and CH_4)/ northern plateau of the Iberian Peninsula (one observatory: Low Atmosphere Research Centre, CIBA)	METEX model, 48-h at 0 m.a.g.l.	Subjective back-trajectory clusters (This study follows Toledano et al. (2009) -They analyse temperatures, distances and average speed		Pérez et al. (2018a)
Atmospheric pollution (CO_2 and CH_4)/ northern plateau of the Iberian Peninsula (one observatory: Low Atmosphere Research Centre, CIBA)	METEX model, 96-h at 500 m.a.g.l.	Objective back-trajectory clusters (Distribution of the regions linked to the groups of trajectory centroids formed from the minima of the density function)	Normalized Difference Vegetation Index (NDVI) and population densities	Pérez et al. (2018b)
Atmospheric pollution (CO_2 and CH_4)/ northern plateau of the Iberian Peninsula (one observatory: Low Atmosphere Research Centre, CIBA)	METEX model, 24-h		Normalized Difference Vegetation Index (NDVI); boundary layer height	Pérez et al. (2019)
Atmospheric pollution (urban plume: CO_2 and CH_4)/ northern plateau of the Iberian Peninsula (one observatory: Low Atmosphere Research Centre, CIBA)	METEX model, 96-h at 500 m.a.g.l.			Fernández-Duque et al. (2020)

The study of back-trajectories in snowfall events on the SE coast of the Iberian Peninsula is of interest due to: 1) the difficulty of measuring this hydrometeor in automatic stations (Buisán et al., 2022); 2) gaps for this hydrometeor in meteorological databases (Enzi et al. 2014) and the lack of previous research studies (Pons et al. 2010, Vicente-Serrano et al. 2017); 3) the exceptional nature of these events in the study area (Capel Molina, 2000a; Martínez-Ibarra et al., 2019), which is one of the warmest and driest regions in continental Europe (Steinhauser, 1970); 4) the use of a database that is partially our own (Martínez-Ibarra et al., 2019); and 5) the fact that very few studies have analysed the back-trajectories of air masses for snowfall events. We have found just two articles: Perry et al. (2007) and Bednorz (2013).

2. Study area

The Iberian Peninsula's location between two continents (Europe and Africa) and two water bodies with opposing characteristics (the Atlantic Ocean and the Mediterranean Sea) produces a large variety of air masses (Pérez et al., 2015). In addition, the complex distribution of its relief implies, among other aspects, a rich variety of climate types, with complex wind patterns, different precipitation regimes and variations in temperature (Capel-Molina, 2000b)

The study area is identified in **Figure 1**. It is located in the SE of the Iberian Peninsula, to be precise in the coastal area of the natural region of SE Iberia, stretching from Benidorm (Alicante) to Adra (Almería) (Gil-Olcina, 2004). The period chosen for our study was 1900-2005. This was because the ECMWF Reanalysis of the 20th Century (ERA-20C) offers data for the period 1900-2010 and the last snowfall event within this period was in 2005. For the purposes of our research into snowfall events over this period, we selected 3 cities considered to be representative of this study area (Alicante, Cartagena and Almería), which have newspaper coverage for the entire period analysed.

Figure 1. Study area.

According to the normal climate values issued by the Spanish Meteorological Office (AEMET) for the period 1981-2010, average annual temperatures oscillate between 17.6-18.3ºC, with average winter temperatures (December-February) ranging between 10.8-13.8ºC, and average minimums in the coldest month (January) of between 5.5-8.3ºC. Together with the coast of Andalusia, it is the warmest part of mainland Spain.

Average annual rainfall is very low at between 200 and 313 mm. It is the driest part of mainland Spain and one of the most arid in continental Europe (Steinhauser, 1970). Snow only fell 25 times in the region in the 118 year-period (1900-2017) for which we reviewed

news reports about snowfalls in the local press (Martínez-Ibarra et al., 2019), i.e. about once every five years on average. As regards snowfall events in which an area is actually covered in snow, these happen approximately once every eight years. In the southernmost area (Almeria), this happens approximately once every 24 years. The period in which there is a risk of snowfall runs from 17th December to 1st April, and the month with most events is January (12 events out of a total of 25).

3. Sources and methodology

The snowfall database used in this research is partially our own. It is explained in detail in Martínez-Ibarra et al. (2019).

The back-trajectories were calculated using the FLEXTRA model. This is a Lagrangian model used to calculate 3D trajectories. It requires the input of high-density meteorological data, where the user can opt for various types of trajectories and change the initial settings (Stohl et al., 1995; Stohl and Seibert, 1998; San José et al., 2005). This model has been used among others by Stohl (1996), Forster et al. (2001), Traub et al. (2003), Gros et al. (2004), Kaiser et al. (2007), Schelfinger and Kaiser (2007), Real et al. (2008), Solberg et al. (2008), Kuhn et al. (2010), Salvador et al. (2010) or Revuelta et al. (2012). The original software is available on this website: https://git.nilu.no/flexpart/flexpart.

The input data for the model comes from the ECMWF Reanalysis of the 20th Century (ERA-20C). Data are available for the period 1900-2010, with analysis every 3 h (although the FLEXTRA model exports this data every 30 minutes) and a spatial resolution of 1.25º (The database was available as free access until June 2023 from the following link: https://www.ecmwf.int/en/forecasts/dataset/ecmwf-reanalysis-20th-century). Other authors normally used a spatial resolution of between 0.5º and 2.5º (0.5º e.g. Fernández-Duque et al., 2020; and 2.5 e.g. Li & Xiao, 2020 or Tosic & Unkasevic, 2013).

3D back-trajectories were considered for just one point in the arrival area, namely, Cartagena, due to its position in the middle of the three points under consideration (Alicante, Cartagena and Almería).

3 levels are usually selected for analysis of the back-trajectories: the first is at the Planetary Boundary Layer (PBL), between 300-500 m.a.s.l.; the second at 850 hPa (1500-2000 m.a.s.l.); and the third from the middle layers at 700-500 hpa (3000-5.000 m.a.s.l.) (Bednorz, 2013; Tosic and Unkasevic, 2013; Hernández-Ceballos et al. 2016; Li & Xiao, 2020; Kleshtanova et al., 2023). With these indications from previous research in mind, we selected 3 levels: 500, 1500 and 5000 m.a.s.l. 500 m.a.s.l. was chosen because various authors considered this the best height from which to track the behaviour of the air masses that circulate under the PBL (Hernández-Ceballos et al. 2016; Domínguez-López et al. 2015; Lozano et al. 2012; Fernández-Duque et al., 2020).

The back-trajectories had a duration of 96 hours (4 days). This is because: 1) 96-hour back-trajectories do not substantially increase the uncertainty associated with their calculation (Ghasemifard et al. 2019; Domínguez-López et al. 2015; Lozano et al. 2012); 2) back-trajectories of shorter duration might not pick up important air-mass sources and routes (Fernández-Duque et al., 2020); 3) 96-hour back-trajectories are sufficient for

analysing the movement of air masses in the Iberian Peninsula and its surrounding area and represent air flows at a synoptic scale (Fernández-Duque et al., 2020); and 4), the calculation of the 96-hour period makes it easier to find out if the air masses have linear trajectories or if they recirculate, which could indicate changes in their initial characteristics and, in short, an increase in their water content (Fernández-Duque et al., 2020) and in moisture sources (Tosic & Unkasevic, 2013). The 96-hour resolution has been used extensively by authors such as: Jorba et al. (2004); Dueñas et al. (2011); Banacos et al. (2010); Izquierdo, Alarcón & Ávila (2013); Tosic & Unkasevic (2013); Pérez et al. (2018b); Fernández-Duque et al. (2020).
Although the trajectories can be grouped into clusters using a numerical calculation method (Jorba et al., 2004; Dueñas et al., 2011; Valenzuela et al., 2012; Baker, 2010; Kassomenos et al., 2010; Izquierdo, Alarcón and Ávila, 2013; Notaro et al., 2013; Notario et al., 2014; Hernández-Ceballos, Brattich and Cinelli, 2016), in this case we used a subjective method. The subjective procedure for trajectory clustering was used, among others, by García et al. (2005), Toledano et al. (2009), Obregón et al. (2012), Saavedra et al. (2012), Tosic and Unkasevic (2013), Pérez et al. (2015), Pérez et al. (2018a) and Kleshtanova et al. (2023).

The first stage was to classify the trajectories according to their direction from their point of origin to their arrival point (N, NE, E, SE, S, SW, W and NW), according to Tosic and Unkasevic (2013). This criterion was not followed in the case of:

1) Short trajectories, in the immediate Iberian Peninsula area. In this case, the back-trajectory was defined as local (L). Proposal inspired by Toledano et al. (2009) and followed by Hernández-Ceballos et al. (2016) and Pérez et al. (2018a).

2) We also considered the type of surface covered by the trajectory, as in Li et al. (2011), Yan and Kim (2012), Avery et al. (2013), Kleshtanova et al. (2023) or Räty et al. (2023). In our research, in line with Trapero et al. (2013) or Pérez et al. (2018a), we were interested in the sea route across the Mediterranean as a possible source of energy and moisture. This is why we differentiated the back-trajectories that covered a mainly Mediterranean route. The decision as to what was their "main route" was taken in part on the basis of the proposal presented by Kleshtanova et al (2023). In our case it was less strict (less than half of its total trajectory), given that our trajectories were longer. Those back-trajectories that followed a mainly Mediterranean route were identified with the abbreviation "MED", in line with the proposals of Toledano et al. (2009) and Pérez et al. (2018a).

3) When the trajectory varied between the different levels, it was referred to as hybrid, in accordance with Tosic and Unkasevic (2013). In those cases, we have specified in brackets the altitude level of the trajectory (or trajectories) in the low Troposphere that diverged from the trajectory at the highest altitude.

Various complementary (secondary) aspects have also been considered:

1) Mediterranean maritime routes at the end of the trajectory: "med" for short trajectories and "meda" for longer ones. Trajectories with a Mediterranean route of at least 25% of the total (≥ 23 hours) were considered long trajectories. We indicate, in brackets, the level(s) that display this characteristic and the length of this route in hours.

2) We also considered the anticyclonic nature of the trajectories, in line with contributions by Banacos et al. (2010). Here, we are referring to whether the back-trajectories border on the Atlantic ridge that is usually present at altitude to the west of western Europe. In these cases, the following code has been added: bar (borders the Atlantic ridge).

3) We also identified back-trajectories with a return (r) component, a consideration inspired by Fernández-Duque et al. (2020).

4) Lastly, we observed whether the trajectory crossed the Strait of Gibraltar, without return (StG) or with return (StGr).

Some additional characteristics have also been considered:

1) The temperatures at the start and finish of the trajectory (t, ºC). A variable considered by Perry et al. (2007) and Pérez et al. (2018a).

2) The altitude at the start and finish of the trajectory, and for 500 m.a.s.l. the evolution of the trajectory over the final stages (a few hundred kilometres before reaching the destination point, to find out whether it was subsiding –sub- or ascending –asc-). This last variable was considered by Perry et al. (2007), Banacos et al. (2010), Tosic and Unkasevic (2013), Trapero et al. (2013) or Tan et al. (2018).

3) The specific humidity at the start and finish (q, gKg^{-1}). The moisture content has often been studied in trajectories analysis to analyse the source or origin of precipitations (Tan et al., 2018), and snowfalls (Perry et al., 2007). In line with Trapero et al. (2013), we also considered this parameter so as to assess the possible role of the Mediterranean as a regional or local source of moisture.

4) The geographic origin of the trajectories was also considered (e.g. Greenland, the North Sea, Slovenia, etc.), as in Pérez et al. (2015), in this case for the three levels being studied.

Our analysis of the trajectories was completed with a synoptic classification as in Banacos et al. (2010), Kirk & Schmidlin (2018) and Pérez et al. (2018a). This was established on the basis of the geopotential altitude in 500 hPa and the pressure on the surface at 12 UTC, as used in various papers on snowfalls in the Iberian Peninsula (Núñez-Mora et al., 2016; De-Pablo-Dávila et al., 2020). These data also came from the ERA-20C. A subjective classification was conducted (expert opinion), a method also applied in other studies of trajectories (e.g. Núñez-Mora et al., 2016). The proposed classification is our own and has never been published. This was performed during the last day of the trajectory, in line with Kirk and Schmidlin (2018), except in exceptional cases, in which during the penultimate day of the trajectory there were Mediterranean maritime flows that were well-defined on the surface. The first stage was to carry out a classification of the map at 500 hPa. Two models or typical situations were found, namely Omega situations and dipoles. Omega situations were grouped according to the direction of the principal axis of the mixed structure: N-S or NE-SW axes. A numerical code was associated with the 500 hPa situations: 1 (Mixed structure N-S), 2 (Mixed structure NE-SW) and 3 (Dipole). We differentiated between ascending and descending branches (asc and des), and their direction (e.g. NW, SW, NE, etc.).
On the surface, two synoptic structures were identified, i.e. dipoles or an isobaric centre that defined the synoptic scenario by itself. 3 situations were displayed: 1) dipole with a

deep anticyclone, situated between the Azores and the Scandinavian Peninsula, and a shallow low situated in the Western Mediterranean. The dipoles were classified on the basis of the position of their main axis, in NE-SW and E-W. The different types were expressed with a numerical code: 1 (Dipole N-S axis); 2 (Dipole NE-SW axis); 3 (Dipole E-W axis); 4 (powerful anticyclone from the Azores); and 5 (a deep low in the Western Mediterranean). We also added a complement reflecting whether or not the wind-flow has a clearly Mediterranean component and if so, whether it has a short (med) or long trajectory (meda). When defining trajectory length, the map of the surface for the day before was also taken into consideration.

These 2 digits were then combined to create the weather types classification (**Table 2**), to which the altitude (type of branch and direction thereof) and surface (if it follows a Mediterranean route) complements were added.

Table 2. Synthesis of the different weather types identified

Synoptic type	Characterization at altitude	Characterization on the surface
1/1	Mixed structure (ridge-trough) main axis N→S	Dipole (anticyclone North Atlantic and low Western Mediterranean) main axis N→S
1/2	Mixed structure (ridge-trough) main axis N→S	Dipole (anticyclone North Atlantic and low Western Mediterranean) main axis NE→SW
1/3	Mixed structure (ridge-trough) main axis N→S	Dipole (anticyclone North Atlantic and low Western Mediterranean) main axis E→W
1/5	Mixed structure (ridge-trough) main axis N→S	Deep Low Western Mediterranean
2/2	Mixed structure (ridge-trough) main axis NE→SW	Dipole (anticyclone North Atlantic and low Western Mediterranean) main axis NE→SW
2/3	Mixed structure (ridge-trough) main axis NE→SW	Dipole (anticyclone North Atlantic and low Western Mediterranean) main axis E→W
2/4	Mixed structure (ridge-trough) main axis NE→SW	Anticyclone of the Azores
3/3	Dipole	Dipole (anticyclone North Atlantic and low Western Mediterranean) main axis E→W

4. Results

4.1 Synoptic analysis

In order to understand the back-trajectories, we began by analysing the synoptic framework. These were categorized as mixed structures at altitude (ridge/trough) with a main NE/SW axis (75% of cases) and dipoles on the surface (91.7% of cases), with anticyclones in the area around the British Isles and weak lows over the Western Mediterranean. There were slightly more ascending branches than descending ones (13

compared to 11). The ascending branches always came from the SW. The descending ones came mainly from the W (NW=7 and W=2), as compared to just two with an eastern component (NE=2).

The dominant synoptic type was 2/2 (12 cases, 50%). The main axis of the structure at altitude maintained a NE/SW orientation, and the mass of cold air was normally expelled over Central Europe. The dipole on the surface also had a main NE/SW axis, and was marked by the presence of a deep Atlantic anticyclone, normally situated around the British Isles, accompanied by weak low pressure over the Western Mediterranean, normally situated between the Balearic Islands and the Italian Peninsula (**Figure 2**).

Figure 2. Centroids of the weather types identified and their frequency of occurrence in %.

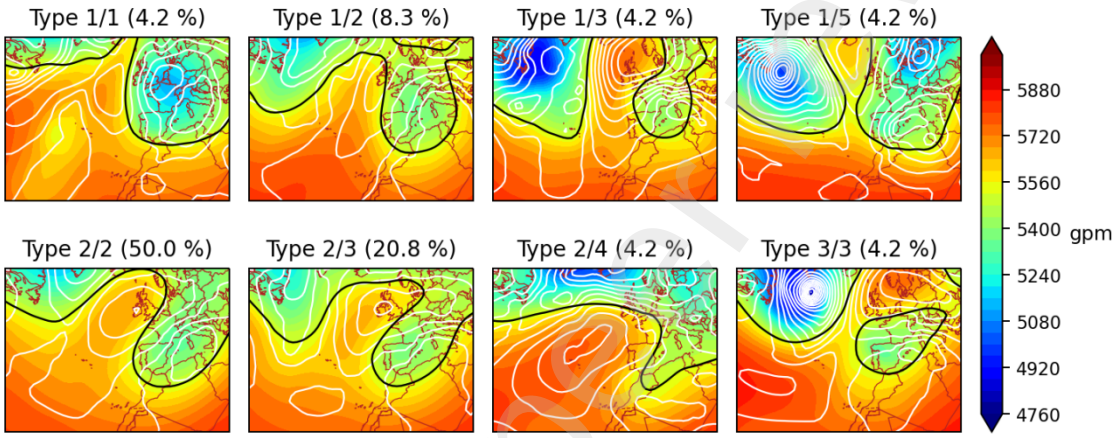

Legend: In each map, the geopotential height at the 500 hPa level is shaded in colour and the isohypse for the standard atmosphere is drawn in black. The isobars for the reduced pressure at sea level are drawn in white.

The second most frequent type was 2/3, with 5 cases (20.8%). It also has a mixed structure with a main NE-SW axis, while on the surface it shows a dipole with a main E-W axis (**Figure 2**). In those cases in which this axis is situated over the Mediterranean Basin, as in 1926, 1971 and 1980, long sea tracks are favoured.

The third most frequent type was 1/2 (2 cases). It is characterized by a mixed structure at altitude with a main N-S axis and a dipole on the surface with a main NE-SW axis (**Figure 2**). The other options (3/3, 2/4 and 1/5) appeared just once. These 3 cases were the result of an evolution or earlier presence of the most frequent situations described above.

4.2 Analysis of the geographic origin of the trajectories

The trajectories at 5000 m.a.s.l. are longer and of more diverse origin (**Figure 3**). Those at 1500 and 500 m.a.s.l. normally have similar area of origin. There was just one episode with a trajectory of local origin (1960 snowfall event) and this occurred exclusively at 1500 and 500 m.a.s.l.

Figure 3. Origin of the trajectories by levels.

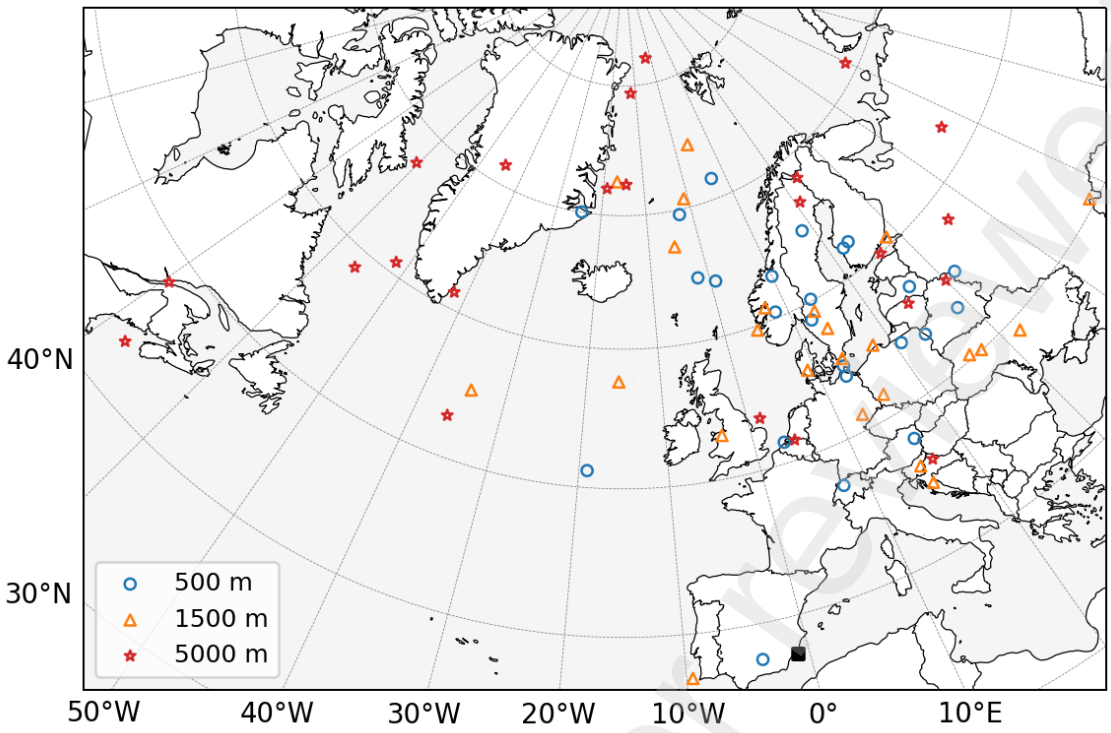

Legend: The blue circles, orange triangles and red stars correspond respectively with the origins of the trajectories at 500, 1500 and 5000 m.a.s.l. The black square over the SE of the Iberian Peninsula marks the location of the end point of all the trajectories we calculated.

In thirteen cases (54.2%) the trajectories at 5000 m.a.s.l. covered very long distances, originating on the eastern coasts of Greenland, the island of Greenland itself, the Labrador Sea, eastern Canada or the north-east coast of the United States. At this level, the general circulation from the west leaves the greatest mark and the need to border the Atlantic ridge that is normally present at altitude to the west of Western Europe. Even in those cases when the trajectories at 5000 m.a.s.l. do not border this anti-cyclonic structure, they may also be associated with long tracks. For example, on two occasions the trajectories originated in the north of the Scandinavian Peninsula and once even in the Barents Sea. The trajectories for 1500 and 500 m.a.s.l did not reach such northerly latitudes over the continent of Europe.

At 1500 m.a.s.l. a greater role is played by the trajectories originating in inland Eastern European countries situated further south (Ukraine and its surrounding area) and the Mediterranean countries from the north of the Adriatic (with 6 cases in total, 25%). Those originating from the Baltic Sea and its surrounding countries (20.8%), the Norwegian Sea-Greenland Sea (16.7%) and the Scandinavian Peninsula (12.5%) also stand out.

The trajectories at 500 m.a.s.l. come especially from the Scandinavian Peninsula (29.2%), and the Norwegian-Greenland Sea (20.8%), as well as from the North Sea and its coastal countries (16.7%) and inland Central European countries (12.5%).

4.3 Classification of trajectories

The trajectories have been grouped into four types: N, NE, NW and hybrids. There were no cases of MED (i.e. in which a main Mediterranean trajectory was observed at all three

levels) (**Figure 4)**. Most of the cases showed NE trajectories (58.3% of the cases). These were followed by hybrids (25%). The N trajectories appeared much more sporadically (12.5%), while the NW trajectories were very rare with just one event. At altitude (5000 m.a.s.l.), the trajectories always displayed a northern component (from NW to NE).

Figure 4. Trajectories by types and their frequency of occurrence in %.

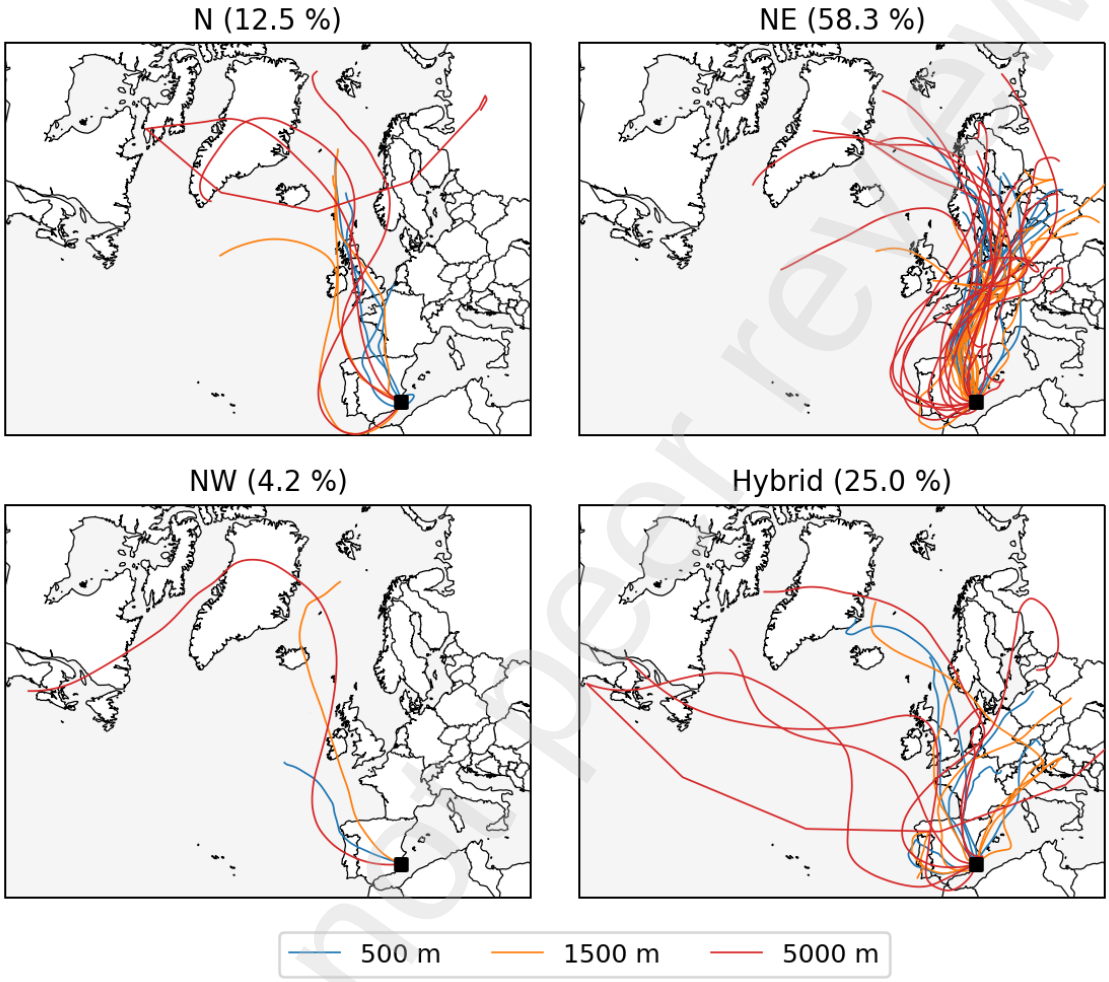

In the hybrid trajectories (n=6), the trajectories were never the same at all three levels: NW/N; NE/MED; N/NW_MED (first NW and then MED in the lower layers); NW/NE; NE/Local; N/MED. Both the Mediterranean and the local trajectories only appeared in the low levels of the troposphere (500 and 1500 m.a.s.l.). There was only one case of a trajectory of local origin.

4.4 Characterization of the trajectories

The average temperatures at the destination point were +2.9ºC (500 m.a.s.l.), -4.4ºC (1.500 m.a.s.l.) and -25.4ºC (5000 m.a.s.l.). Between the start and finish of the trajectory, the temperature increased on average by +12.6º at 500 m.a.s.l., ≈+6º at 1500 m.a.s.l. and 5000 m.a.s.l. (**Tables 3, 4 and 5**). For the specific cases, the most striking increases, of over 20ºC, also occurred more frequently at 500 m.a.s.l. (5 cases at 500 m.a.s.l. and just one case at 1500 m.a.s.l. and at 5000 m.a.s.l.). The five cases at 500 m.a.s.l. share a common trajectory that crosses the Iberian Peninsula and its cordilleras: in most cases the Cantabrian Mountains-Pyrenees and later the Sistema Ibérico; and failing that the

Alicante-Murcia branch of the Betic Cordillera. They also share the fact that they subside in the last part of their journey, normally from the Iberian System onwards.

At 500 m.a.s.l. there was only one case in which the temperature fell between the start and finish of the trajectory (Δ -1.13 on 9th January 1945). This event coincided with one of the two trajectories that did not begin with a cold front. The trajectory originated over the North Atlantic to the west of the southern part of the British Isles.

Falls in temperature were more common at 5000 m.a.s.l. and 1500 m.a.s.l.: 5 cases at 5000 m.a.s.l. and 6 cases at 1500 m.a.s.l. The average values, filtering the increases and decreases separately, were: Δ -3.7 at 1500 m.a.s.l. and Δ -2.8 at 5000 m.a.s.l.; and $\Delta + 9.4$ at 1500 m.a.s.l. and $\Delta + 8.3$ at 5000 m.a.s.l.

The specific humidity values (q) at the end of the trajectories were very similar at 500 m.a.s.l. and 1500 m.a.s.l.: $\overline{q}$=2.7 gKg^{-1} [1-5,4 gKg^{-1}] at 500 m.a.s.l.; and $\overline{q}$=2.1 gKg^{-1} [1-4 gKg^{-1}] at 1500 m.a.s.l. At 5000 m.a.s.l. they were much lower: $\overline{q}$=0.3 gKg^{-1} [0.028 to 1.2 gKg^{-1}]. The values at 500 m.a.s.l. and 1500 m.a.s.l. were normally quite similar except in the 1960 event. If we do not take this episode into consideration, the R^2 between the two levels was 0.8404 (n=23). The dissimilar event from 1960 was also the only event with a trajectory of local origin at 500 m and 1500 m.

Table 3. Characterization of the trajectories at 500 m.a.s.l.

Date	z_0	z_1	Δz	Δz final stage	t_0	t_1	ΔT	q_0	q_1
19020131	500	253.9	246.1	Subsidence	3.7	-8.2	11.9	2.5	1.1
19100401	500	1034.5	-534.5	Subsidence	3.5	-3.4	7.0	3.3	2.3
19140101	500	605.1	-105.1	Subsidence	0.8	-19.1	19.9	1.9	0.57
19170324	500	259	241.0	Subsidence	6.4	4.1	2.3	2.9	4.5
19190124	500	1107.4	-607.4	Subsidence	7.2	-5.9	13.1	4.2	2.2
19261225	500	401.5	98.5	Subsidence	4.1	-15.9	20.1	1.8	0.98
19331217	500	276.6	223.4	Subsidence	2.5	-8.3	10.8	2	1.1
19340202	500	723.3	-223.3	Subsidence	2.3	-23.5	25.9	2.5	0.36
19350131	500	493.7	6.3	Subsidence	2.7	-11.3	14.1	2.7	0.98
19350209	500	846.8	-346.8	Subsidence	1.7	-10.4	12.1	3.1	1.6
19390319	500	362.4	137.6	Subsidence	2.3	-2.3	4.6	2.3	1.6
19450109	500	268.7	231.3	Subsidence	4.5	5.6	-1.1	2.8	3.7
19460117	500	338.6	161.4	Ascendance	3.1	-16.2	19.4	3.5	0.85
19540203	500	335.3	164.7	Subsidence	2.6	-23.4	25.9	2.5	0.45
19560211	500	430	70.0	Subsidence	-2.9	-26.4	23.5	1.1	0.34
19570116	500	358	142.0	Subsidence	2.1	-8.0	10.2	2.4	1.8
19600111	500	914.5	-414.5	Subsidence	10.7	8.5	2.2	5.4	5
19621225	500	388.2	111.8	Subsidence	2.1	-20.7	22.8	1.8	0.6
19710308	500	277.6	222.4	Subsidence	4.2	-9.7	13.9	3.7	0.86
19800113	500	679.3	-179.3	Subsidence	3.2	-5.0	8.2	4	2.4

19830212	500	294.5	205.5	Ascendance	1.0	-1.9	2.9	3.6	2.3
19850115	500	306	194.0	Subsidence	-3.5	-18.8	15.3	1.3	0.73
20040301	500	257	243.0	Subsidence	5.3	-7.4	12.7	2.6	0.87
20050127	500	262.1	237.9	Subsidence	-0.8	-5.7	4.9	1.6	1.7
	Averages	**478.1**	**21.9**		**2.9**	**-9.7**	**12.6**	**2.7**	**1.6**

Table 4. Characterization of the trajectories at 1500 m.a.s.l.

Date	z_0	z_1	Δz	t_0	t_1	ΔT	q_0	q_1
19020131	1500	1195.4	304.6	-3.1	-22.0	18.9	1.6	0.45
19100401	1500	1418.1	81.9	-4.9	-7.3	2.4	2.9	2.5
19140101	1500	1233.7	266.3	-6.5	-16.7	10.2	1.1	0.64
19170324	1500	1948.4	-448.4	-3.5	-2.8	-0.7	2.6	1.6
19190124	1500	1675	-175.0	-0.2	-6.3	6.1	3.3	2.6
19261225	1500	1420	80.0	-4.3	-10.1	5.8	1.5	1.9
19331217	1500	1434.6	65.4	-5.2	-19.9	14.8	1.3	0.55
19340202	1500	1145.5	354.5	-5.0	-26.2	21.2	2.2	0.25
19350131	1500	1259	241.0	-4.5	-12.7	8.2	2.6	1.3
19350209	1500	1392.3	107.7	-5.0	-3.7	-1.3	2.8	2.9
19390319	1500	1309.2	190.8	-6.9	-1.2	-5.7	1.9	4
19450109	1500	1242.5	257.5	-3.6	-10.7	7.1	1.5	1.1
19460117	1500	1243	257.0	-3.7	-14.8	11.1	2.8	1
19540203	1500	1415.1	84.9	-1.6	-18.5	16.9	2.2	0.56
19560211	1500	1299.7	200.3	-8.3	-12.5	4.2	0.84	1.4
19570116	1500	1473.9	26.1	-4.0	-4.1	0.1	1.8	2.6
19600111	1500	1323.4	176.6	4.1	10.3	-6.2	1.4	2
19621225	1500	1376.6	123.4	-5.2	-11.1	6.0	1.5	0.95
19710308	1500	1469.5	30.5	-3.1	-20.7	17.5	3.3	0.71
19800113	1500	1548.9	-48.9	-2.6	-8.5	5.9	3.6	1.8
19830212	1500	1320.7	179.3	-5.7	2.1	-7.8	2.5	4
19850115	1500	1387.6	112.4	-11.0	-10.3	-0.7	0.77	1.6
20040301	1500	1215.8	284.2	-4.4	-17.7	13.2	2.5	0.86
20050127	1500	1299.6	200.4	-8.7	-9.0	0.3	1.7	1.8
	Averages	**1377.0**	**123.0**	**-4.4**	**-10.6**	**6.2**	**2.1**	**1.6**

Table 5. Characterization of the trajectories at 5000 m.a.s.l.

Date	z_0	z_1	Δz	t_0	t_1	ΔT	q_0	q_1
19020131	5000	4813.9	186.1	-19.7	-30.3	10.6	0.100	0.440
19100401	5000	4883.2	116.8	-20.0	-18.2	-1.8	0.580	1.400
19140101	5000	4664.6	335.4	-28.0	-36.1	8.1	0.140	0.081
19170324	5000	4584.8	415.2	-21.7	-33.6	11.9	0.230	0.130
19190124	5000	4816.8	183.2	-19.8	-21.2	1.3	0.087	1.000

19261225	5000	4935.1	64.9	-30.0	-34.7	4.8	0.370	0.280
19331217	5000	4608.9	391.1	-24.2	-30.9	6.7	0.140	0.190
19340202	5000	4520.7	479.3	-32.6	-41.2	8.7	0.260	0.066
19350131	5000	6066.8	-1066.8	-22.6	-46.5	23.9	0.140	0.070
19350209	5000	4707	293.0	-31.7	-32.3	0.5	0.210	0.220
19390319	5000	4760.3	239.7	-25.6	-30.1	4.5	0.087	0.410
19450109	5000	4876.8	123.2	-24.9	-23.7	-1.1	0.072	0.790
19460117	5000	4557.7	442.3	-19.2	-38.1	18.9	0.033	0.110
19540203	5000	4932.7	67.3	-20.5	-24.9	4.4	1.200	0.610
19560211	5000	5088.9	-88.9	-22.1	-25.2	3.1	0.028	0.470
19570116	5000	4906.1	93.9	-27.7	-21.7	-6.0	0.390	0.730
19600111	5000	4762.5	237.5	-25.3	-29.0	3.7	0.100	0.380
19621225	5000	4707.5	292.5	-25.8	-37.0	11.2	0.390	0.200
19710308	5000	4752.6	247.4	-26.6	-24.3	-2.3	0.520	0.160
19800113	5000	4753.3	246.7	-25.6	-34.1	8.5	0.580	0.120
19830212	5000	4812.2	187.8	-30.3	-36.2	5.9	0.320	0.230
19850115	5000	4926.8	73.2	-32.8	-30.0	-2.7	0.079	0.230
20040301	5000	4520	480.0	-20.9	-36.8	15.9	0.130	0.100
20050127	5000	4963	37.0	-32.6	-37.6	5.0	0.320	0.140
	Averages	**4830.1**	**169.9**	**-25.4**	**-31.4**	**6.0**	**0.271**	**0.357**

At 500 m.a.s.l. we analysed the situations with the greatest moisture content (90th percentile) in the study area. There were 3 events with higher levels of specific humidity ranging between 4 and 5.4 gKg^{-1} (q[4-5.4 gKg^{-1}]): 2 of these events also coincided with the 90th percentile at 1500 m.a.s.l.; and in one situation with a 90th percentile at 5000 m.a.s.l.. Situations of this kind are normally related with hybrid trajectories with long sea tracks in the lower layers, from the Adriatic Sea, coinciding with synoptic structures on the surface that also enable wind flows with long Mediterranean tracks.

We also studied the changes in altitude at the start and finish of the trajectories and at the end of the episode. On average, the difference between the start and finish altitudes was positive: at 1500 m.a.s.l. the end point was 120 m higher than the start point while at 5000 m.a.s.l. the difference was 170 m. At 500 m.a.s.l. the difference was much smaller (22 m). Of the 6 most pronounced ascents at 500 m.a.s.l. (in the region of or above the 90th percentile), 4 also showed significant increases at 1500 m.a.s.l. and 3 at 5000 m.a.s.l.

In the 2004 event, there were ascents in excess of the 90th percentile at all three levels. This event coincided with a trajectory from the North, with a long track, from the Arctic Ocean at 5000 m.a.s.l. and from the Greenland Sea at 500 and 1500 m.a.s.l., with the most common weather type, 2/2.

There were only two descents in altitude at 5000 m.a.s.l. (although one of these was very pronounced: Δ-1067 m) and 3 at 1500 m.a.s.l. (one of which was pronounced: Δ-448 m). At 500 m.a.s.l. they were more frequent, with a total of 7 (29% of cases); three of these were less than -400 m. There were just two occasions on which descents between the start

and finish of the trajectory were recorded at different levels. On both occasions, this was at 500 and 1500 m.a.s.l.

The most important descent in the trajectories was on 31st January 1935, on which there was a descent of -1067 m at 5000 m.a.s.l. This coincided with the greatest increase in temperature at 5000 m.a.s.l. (Δ+23.9ºC). This was related with the fact that this trajectory, which originated on the Greenland Ice Sheet, had the highest initial altitude (6067 m.a.s.l.).

The most important descent in altitude at 500 m.a.s.l. (Δ -607.4 m) took place in January 1919. It coincided with the second most significant descent at 1500 m.a.s.l. (Δ -175). It was related with a high start of trajectory, the highest at 500 m.a.s.l. (1107 m, when the average was just 478 m); and the second highest at 1500 m.a.s.l. (1675 m.a.s.l., compared to an average of 1377); both these trajectories (for 500 and 1500 m.a.s.l.) originated in a country in the Alpine arc, namely Switzerland and Slovenia respectively.

During the final stage of the trajectory at 500 m.a.s.l. the altitude curve was characterized by subsidence (92% of cases, 22 out of 24 occasions), mostly from the Iberian System onwards (19 cases). The two cases in which there was ascent at the end of the trajectories at 500 m.a.s.l. were linked with final tracks across the Mediterranean (23 and 25.5 hours of the trajectory), and ascents of about 200 m, with winds on the surface with a long Mediterranean track and absolute humidity values that were close to the 90th percentile at 500 m.a.s.l. These also coincided with ascending branches at altitude (500 hPa) with an SW component.

4.5 Relationship between trajectories and weather types

The relationship between the type of trajectory and the synoptic situations was affected by the dominance of NE trajectories and the high frequency of 2/2 weather types. 50% of the NE trajectories (n=14) were identified with the 2/2 weather type, and 85.7% were identified with a type 2 at altitude. The hybrid trajectories (n=6) were also identified with 2/2 weather types (50%), although the identification with a type 2 at altitude was not so high as for the NE trajectories (66.7%). Weather type 2/2 was even important in the N trajectories (n=3) (2 out of 3 cases). The only NW trajectory analysed was not related with the dominant weather type (2/2), but with situation 1/1.

5. Discussion

As in the article by Kirk & Schmidlin (2018), the analysis of the synoptic classification during the last day of the trajectory was useful for identifying air-mass corridors, in particular in the back-trajectories at 5000 m.a.s.l. Furthermore, the number of synoptic patterns identified (8) for this type of event (snowfall) was similar to those identified in other parts of the Iberian Peninsula (e.g. Núñez-Mora et al., 2016; or De-Pablo-Dávila et al., 2020), and in particular to those identified by Esteban et al. (2005) and Ortega & Morales (2022).

It is also important to highlight the clear similarity between the synoptic patterns identified here and those proposed in other studies. In the Valencia region of Spain, Núñez-Mora et al. (2016), proposed 3 similar types to ours: their group 1 coincided with our type 1/5; their group 2 with our 2/4; and their group 4 with our 1/1. In a study of the

most intense snowfalls in the coastal provinces of the Cantabrian Sea by De-Pablo-Dávila et al. (2020), their most frequent synoptic pattern is similar to our most common scenario, 2/2. Similarly, in research by Ortega & Morales (2022) on snowfalls in inland northern areas of the Iberian Peninsula (Castilla y León; 1979-2021), 3 of the weather types they proposed were similar to ours: the "mA trough" to the East is similar to our 1/1; the "cP shear line" is similar to 2/2; while the "cP cold centered" is similar to 2/3. Even, for a part of the Peninsula with a very different climate from our study area (Andorra, Pyrenees), the Cluster 2 proposed by Esteban et al., (2005) for events with strong snowfalls is identical to our most frequent weather type (2/2).

The number of back-trajectory patterns identified and their characteristics are similar to those reported in previous research. For example, we have obtained a group of trajectories similar to those obtained by Perry et al. (2007) in a study of snowfalls in the SE of the Appalachian Mountains (United States) (n=191; back-trajectories of 72h). These authors established 5 groups of trajectories at a more general level of classification and 7 more detailed second-level groups; while we identified 4 groups at the first general level and 8 at the second level. By contrast, they are slightly lower than those established for extreme snowfall events in Belgrade (Serbia) by Tosik & Unkasevic (2013): 8 at the first level and 13 at the second. Our first-level classification could therefore be regarded as a lower-intermediate classification (Pérez et al., 2015), sufficient for analysing air-mass penetration paths i.e. the origin and the path followed by the trajectories at a synoptic scale (Pérez et al., 2015), especially when the second-level distinction is permitted in complex (hybrid) situations. It is also important to highlight the similarity between one of the trajectories that caused the intense snowfall events in Bremen (NE Germany) (Bednorz, 2013) with those that we identified. In particular, those that come from the North with a geographic origin in the Greenland Sea.

The temperatures associated with snowfalls in our study area are related with powerful influxes of cold air at 850 hPa. Temperatures are normally around -5 ºC or slightly lower. This situation was also noted for example in the island of Mallorca (Spain) (Salamanca-Salamanca et al. 2012); Athens (Houssos et al. 2007); the Côte d'Azur and the island of Corsica (Goulet 2017); in the most common scenario for snowfalls in the coastal provinces of the northern part of the Iberian Peninsula (De-Pablo-Dávila et al., 2020); even in the north and centre of Europe (Bednorz, 2013).

The humidity conditions associated with these events are similar to those obtained by Perry et al (2007) in a study of the Appalachian Mountains. These authors obtained similar mixing ratio thresholds (which can be approximated by the specific humidity) [1.72-2.66] to those observed in our study ($\overline{q}$=2.1 gKg-1 [1-4 gKg-1]).

Lastly, we should emphasize the importance of the Mediterranean Sea as a source of humidity, even in areas a long way from its basin. This was demonstrated for example by Bednorz (2013) in a study of the back-trajectories (-48h) in most of the intense snowfalls in Smolensk (in Eastern Russia near the border with Belarus). The Mediterranean has also been shown to have played an important role in snowfalls in Budapest (Bednorz, 2013) and in general, in extreme precipitation events in the south and east of Europe (Tosik & Unkasevic, 2013). In our case, in general, the trajectories with the longest Mediterranean tracks have been related with noteworthy events. For example: 1) the snowfall event of

1946, which covered the ground in Cartagena (Murcia) and El Campello (Alicante), with a long trajectory across the Mediterranean of 25.5 hours at z=500 m.a.s.l.; 2) the episode of 1957, with a 26.5-h trajectory across the Mediterranean at z=5000 m.a.s.l. On that occasion, the snow settled in the city of Alicante; or 3) the 1971 episode, with a 34-h trajectory across the Mediterranean at z=1500 m.a.s.l. and 29 h at z=500 m.a.s.l. On that occasion the snow settled in La Manga del Mar Menor in Murcia.

6. Conclusions

This subjective synoptic study and analysis of back-trajectories has enabled us to advance in the atmospheric characterization of snowfall events on the southeast coast of the Iberian Peninsula.

Most of these episodes were related with the presence of mixed structures at altitude (ridge/trough), with a main NE-SW axis, and dipoles on the surface with a main NE-SW axis characterized by the presence of powerful North Atlantic anticyclones situated in the area around the British Isles and lows in the western Mediterranean, in this case quite shallow. These scenarios have coincided in most cases with trajectories from the NE at the three levels analyzed (500, 1500 and 5000 m.a.s.l.).

As regards the geographic origin of the trajectories, there were differences between the 5000 m.a.s.l. level and the two levels from the low troposphere (500 and 1500 m.a.s.l.). The trajectories at 5000 m.a.s.l. had a more distant source. They often crossed the entire North Atlantic Ocean, bordering the anticyclonic ridge situated to the west of Western Europe. By contrast, those at 500 and 1500 m.a.s.l. had quite similar. Most originated in Central and Eastern Europe, Scandinavian countries or the Norwegian Sea. On one occasion, they both showed local origin.

As was expected, over the course of the trajectory, the particles undergo a process of denaturalization, especially at the level that is most influenced by the Earth's surface (z=500 m.a.s.l.). This process was characterized above all by an increase in temperature of over 12ºC (on average) at this level. However, the increase in the moisture content was relatively insignificant even at 500 m.a.s.l. (+1.11 g/Kg). This means that neither the long Mediterranean tracks nor the local trajectories in the low troposphere managed to increase their specific humidity values at 500 m.a.s.l. above the maximum of 5.4 g/Kg.

Although between the start and finish points of the trajectories, the particles at all three levels normally ascended in altitude, the situation in the low troposphere (z=500 m.a.s.l.) was characterized by subsidence in the final stage of the trajectory, once it had passed the reliefs in the northern half of the Iberian Peninsula. Ascents and higher humidity values than normal at the end of the trajectory were only recorded in some of the trans-Mediterranean tracks with meteorological situations on the surface dominated by Mediterranean winds with a long sea track.

References

Adame, J.A., Hernández-Ceballos, M.A., Bolívar, J.P., De la Morena, B. 2012b. Assessment of an air pollution event in the southwestern Iberian Península. Atmos. Environ. 55, 245-256. https://doi.org/10.1016/j.atmosenv.2012.03.010.

Adame, J.A., Notario, A., Villanueva, F., Albaladejo, J. 2012a. Application of cluster analysis to surface ozone, NO2 and SO2 daily patterns in an industrial area in Central-Southern Spain measured with a DOAS system. Sci. Total Environ. 429, 281-291. https://doi.org/10.1016/j.scitotenv.2012.04.032.

Asaf, D., Pedersen, D., Peleg, M., Matveev, V., Luria, M. 2008. Evaluation of background levels of air pollutants over Israel. Atmos. Environ. 42(36), 8453-8463. https://doi.org/10.1016/j.atmosenv.2008.08.011

Avery, Jr., G.B., Biswas, K.F., Mead, R., Southwell, M., Willey, J.D., Kieber, R.J., M ullaugh, K.M. 2013. Carbon isotopic characterization of hydrophobic dissolved organic carbón in rain water. Atmos. Environ. 68, 230-234. https://doi.org/10.1016/j.atmosenv.2012.11.054.

Baker, J. 2010. A cluster analysis of long range air transport pathways and associated pollutant concentrations within the UK. Atmos. Environ. 44, 563-571. https://doi.org/10.1016/j.atmosenv.2009.10.030.

Banacos, P. C., Ekster, M. L. 2010. The association of the elevated mixed layer with significant severe weather events in the northeastern United States. Weather Forecast. 25(4), 1082-1102. https://doi.org/10.1175/2010WAF2222363.1.

Bednorz, E. 2004. Snow cover in Eastern Europe in relation to temperature, precipitation and circulation. Int. J. Climatol. 24, 591-601. https://doi.org/10.1002/joc.1014.

Bednorz, E. 2013. Synoptic conditions of heavy snowfalls in Europe. Geogr. Ann. A: Phys. Geogr. 95(1), 7-78. https://doi.org/10.1111/geoa.12001

Buisan, S.T., López-Moreno, J. I., Saz, M.A., Kochendorfer, J. 2016. Impact of weather type variability on winter precipitation, temperature and annual snowpack in the Spanish Pyrenees. Climate Res. 69,79-92. https://doi.org/10.3354/cr01391

Buisan, S.T., Saz, M.A, López-Moreno. J.I. 2015. Spatial and temporal variability of winter snow and precipitation days in the western and central Spanish Pyrennes. Int J Climatol. 35, 259-274. https://doi.org/10.1002/joc.3978

Buisán, S.T., Serrano-Notivoli, R. Kochendorfer, J. and Bello-Millán, F. J. (2022). Adjustment of Solid Precipitation during the Filomena Extreme Snowfall Event in Spain. From Observations to "True Precipitation". B Am. Meteorol. Soc. 103(11), E2570-E2578. https://doi.org/10.1175/BAMS-D-22-0012.1.

Bulygina, O., Razuvaev, V. and Korshunova, N. 2009. Change in snow cover over northern Eurasia in the last decades. Environ. Res. Lett. 4, 045026. https://doi.org/10.1088/17489326/14/4/045026.

Calvo, F. 2000. Panorama de los estudios sobre riesgos naturales en la Geografía espanola. Boletin de la Asoc. de Geogr. Espanoles. 30(1), 21-35.

Capel Molina, J. J. 2000b. El Clima de la Península Ibérica. Editorial Ariel, Colección Ariel Geografía, Barcelona.

Capel-Molina, J.J. 2000a. La nieve y su distribución espacial en la Península Ibérica. Nimbus. Rev. Climat. Meteorol. Paisaje. 5-6, 6-12.

Chen, B., Xu, X.-D., Yang, S., Zhang, W. 2012. On the origin and destination of atmospheric moisture and air mass over the Tibetan Plateau. Theor. Appl. Climatol. 110(3), 423-435. 10.1007/s00704-012-0641-y

Chubb, T. H., Siems, S. T., Manton, M. J. 2011. On the decline of wintertime precipitation in the Snowy Mountains of Southeastern Australia. J. Hydrometeorol. 12(6), 1483-1497. https://doi.org/10.1175/JHM-D-10-05021.1.

Croce, P., Formichi, P., Landi, F. 2021. Extreme ground snow loads in Europe from 1951 to 2100. Clim. 9(9), 133. https://doi.org/10.3390/cli9090133.

Dafis, S., Lolis, C.J., Houssos, E.E., Bartzokas, A. 2016. The atmospheric circulation characteristics favouring snowfall in an area with complex relief in northwestern Greece. Int. J. Climatol. 36, 3561-3577. https://doi.org/10.1002/joc.4576

Datta, A., Saud, T., Goel, A., Tiwari, T., Sharma, S.K., Saxena, M., Mandal, T.K. 2010. Variation of ambient SO2 over Delhi. J. Atmos. Chem. 65(2-3), 127-143. https://doi.org/10.1007/s10874-011-9185-2.

Dauphiné, A. 1972. Les chutes de neige sur le litoral méditerranéen du Sud-Est français. Méditerranée. 11,141-157.

de Pablo D´avila, F., Rivas Soriano, L.J., Jiménez Alonso, C., Mora García, M., Riesco Martín, J. 2021. Synoptic patterns of severe hailstorm events in Spain. Atmos. Res. 250, 105397.https://doi.org/10.1016/j.atmosres.2020.105397

De Pablo-Dávila, F., Rivas-Soriano, L.J., Mora-García, M., Gónzalez-Zamora, A. 2021. Characterization of snowfall events in the northern Iberian Peninsula and the synoptic classification of heavy episodes (1988–2018). Int. J. Climatol. 41, 699-713. https://doi.org/10.1002/joc.6646.

Domínguez-López, D., Vaca, F., Hernandez-Ceballos, M.A., Bolívar, J.P. 2015. Identification and characterisation of regional ozone episodes in the southwest of the Iberian Peninsula. Atmos. Environ. 62, 208-219. http://dx.doi.org/10.1016/j.atmosenv.2012.08.016.

Draxler, R. R. 1992. Hybrid single-particle lagrangian integrated trajectories (HY-SPLIT): Version 3.0-User's Guide and Model Description. NOAA Technical Memo ERL. ARL-195. Air Resources Laboratory (NOAA), Silver Spring.

Draxler, R.R., Stunder, B., Rolph, G., Stein, A., Taylor, A., Zinn, S., Loughner, Ch., Crawfort, A. 2023. Hysplit 5.3 user Guide. Air Resources Laboratory (NOAA), Silver Spring.

Drumond, A., Nieto, R., Gimeno, L., Vicente-Serrano, S. M., López-Moreno, J. I., Morán-Tejeda, E. 2011. Characterization of the atmospheric component of the winter hydrological cycle in the Galicia/North Portugal Euro-region: a Lagrangian approach. Clim. Res. 48(2-3), 193-201. https://doi.org/10.3354/cr00987.

Dueñas, C. Orza, J.A.G, Cabello, M., Fernández, M.C., Cañete, S., Pérez, M., Gordo, E. 2011. Air mass origin and its influence on radionuclide activities (7Be and 210Pb) in

aerosol particles at a coastal site in the western Mediterranean. Atmos. Res. 101, 205-214. https://doi.org/10.1016/j.atmosres.2011.02.011.

Engel, I., Luo, B. P., Pitts, M. C., Poole, L.R., Hoyle, C.R., Grooß, J.-U., Dörnbrack, A., Peter, T. 2013. Heterogeneous formation of polar stratospheric clouds—part 2: nucleation of ice on synoptic scales. Atmos. Chem. Phys. 13(21), 0769-10785. https://doi.org/10.5194/acp-13-10769-2013

Enzi, S., Bertolin, C., Diodato, N. 2014. Snowfall time-series reconstruction in Italy over the last 300 years. Holocene. 24(3), 346-356. https://doi.org/10.1177/0959683613518.

Escudero, M., Stein, A., Draxler, R. R., Querol, X., Alastuey, A., Castillo, S., and Avila, A. 2006. Determination of the contribution of northern Africa dust source áreas to PM10 concentrations over the central Iberian Peninsula using the Hybrid Single-Particle Lagrangian Integrated Trajectory model (HYSPLIT) model. J. Geophys. Res. 111, D06210. https://doi.org/10.1029/2005JD006395.

Esteban, P., Jones, P.D., Martín-Vide, J., Mases, M. 2005. Atmospheric circulation patterns related to heavy snowfall days in Andarra, Pyrennees. Int. J. Climatol. 25, 319-329.https://doi.org/10.1002/joc.1103.

Esteve, A.R., Estellés, V., Segura, S., Utrillas, M.P., Martínez-Lozano, J.A. 2012. Influencia de la trayectoria de las masas de aire en las medidas in situ de las propiedades de los aerosoles en Valencia. Tethys. 9, 35-41. https://doi.org/10.3369/tethys.2012.9.04

Falarz, M. 2007. Snow cover variability in Poland in relation to the macro- and mesoscale atmospheric circulation in the 20th century. Int. J. Climatol. 27, 2069-2081. https://doi.org/10.1002/joc.1505.

Feingold, G., Eberhard, W. L., Veron, D. E., Previdi, M. 2003. First measurements of the Twomey indirect effect using groundbased remote sensors. Geophys. Res. Lett. 30(6), 1287. https://doi.org/10.1029/2002GL016633.

Fernández-Duque, B., Pérez, I. A., García, M. Á., Pardo, N., Sánchez, M. L. 2020. Statistical urban plume analysis using observations and air mass modelling at a rural station in the northern Spanish plateau. Air Qual. Atmos. Hlth. 13, 1343-1350. https://doi.org/10.1007/s11869-020-00889-5.

Fernández-Rodríguez, S., Skjøth, C.A., Tormo-Molina, R., Brandao, R., Caeiro, E., Silva-Palacios, I., Gonzalo-Garijo, A. y Smith, M. 2014. Identification of potential sources of airborne Olea pollen in the Southwest Iberian Peninsula. Int. J. Biometeorol. 58, 337-348. https://doi.org/10.1007/s00484-012-0629-4.

Fita, L., Romero, R., Luque, A., Ramis, C. 2009. Effects of assimilating precipitation zones derived from satellite and lightning data on numerical simulations of tropical-like Mediterranean storms. Ann. Geophys. 27(8), 3297-3319. https://doi.org/10.5194/angeo-27-3297-2009

Forster, C., Wandinger, U., Wotawa, G., James, P., Mattis, I., Althausen, D., Simmonds, P., O'Doherty, S., Jennings, S.G., Kleefeld, C., Schneider, J., Trickl, T., Kreipl, S., Jager, H., Stohl, A. 2001. Transport of boreal forest fire emissions from Canada to Europe. J. Geophys. Res. Atmos. 106, 22887-22906. https://doi.org/10.1029/2001JD900115.

Frei, A., Robinson, D.A. 1999. Northern Hemisphere snow extents. Regional variability 1972–1994. Int. J. Climatol. 19, 1535-1560.

García, M.A., Sánchez, M.L., Pérez, I.A., de Torre, B. 2005. Ground level ozone concentrations at a rural location in northern Spain. Sci. Total Environ. 348, 135-150. https://doi.org/10.1016/j.scitotenv.2004.12.049

García-Lastra, R., Leginagoikoa, I., Plazaola, J.M., Ocabo, B., Aduriz, G., Nunes, T., Juste, R.A. 2012. Bluetongue Virus Serotype 1 Outbreak in the Basque Country (Northern Spain) 2007–2008. Data Support a Primary Vector Windborne Transport. PLoS ONE. 7(3). e34421. https://doi.org/10.1371/journal.pone.0034421.

Ghasemifard, H., Yuan, Y., Luepke, M., Schunk, Ch., Chen, J., Ries, L., Leuchner, M., Menzel, A. 2019. Atmospheric CO 2 and δ13 C Measurements from 2012 to 2014 at the Environmental Research Station Schneefernerhaus, Germany: Technical Corrections, Temporal Variations and Trajectory Clustering. Aerosol Air Qual. Res. 19, 657-670. https://doi.org/10.4209/aaqr.2018.01.0010.

Gil-Olcina, A. 2004. La región climática del sureste ibérico, in: Gil-Olcina A, Morales Gil A, Torres-Alfosea FJ (Eds.), Aridez, salinización y agricultura en el Sureste Ibérico. Fundación Ramón Areces, Madrid, pp. 13-35.

Goulet, L. 2017. The ingredients of snow episodes over southeastern France. European Forecaster. 22-31.

Gros, V., Williams, J., Lawrence, M.G., von Kuhlmann, R., van Aardenne, J., Atlas, E., Chuck, A., Edwards, D.P., Stroud, V., Krol, M. 2004. Tracing the origin and ages of interlaced atmospheric pollution events over the tropical Atlantic Ocean with in situ measurements, satellites, trajectories, emission inventories, and global models. J. Geophys. Res. 109, D22306. https://doi.org/10.1029/2004JD004846.

Harpaz, T., Ziv, B., Saaroni, H., Beja, E. 2014. Extreme summer temperatures in the East Mediterranean-dynamical analysis. Int. J. Climatol. 34(3), 849-862. https://doi.org/10.1002/joc.3727.

Henderson, G.R., Leathers, D.J. 2010. European snow cover extent variability and associations with atmospheric forcing. Int. J. Climatol. 30, 1440-1451. https://doi.org/10.1002/joc.1990.

Hernández-Ceballos, M. A., Adame, J. A., Bolívar, J. P., de la Morena, B. A. 2013. Vertical behaviour and meteorological properties of air masses in the Southwest of the Iberian Peninsula (1997–2007). Meteor. Atmos. Phys. 119(3-4), 163-175. https://doi.org/10.1007/s00703-012-0225-5

Hernández-Ceballos, M. A., Brattich, E., Cinelli, G. 2016. Heat-Wave Events in Spain: Air Mass Analysis and Impacts on 7Be Concentrations. Adv. Meteorol. 8026018. http://dx.doi.org/10.1155/2016/802601

Hernández-Ceballos, M.A., De Felice, L. 2019. Air mass trajectories to estimate the "most likely" areas to be affected by the release of hazardous materials in the atmosphere-feasibility study. Atmosphere. 10, 253. https://doi.org/10.3390/atmos10050253.

Hernández-Ceballos, M.A., Soares, J., García-Mozo, H., Sofiev, M., Bolivar, J.P., Galán, C. 2014. Analysis of atmospheric dispersion of olive pollen in southern Spain using SILAM and HYSPLIT models. Aerobiologia. 30, 239-255. https://doi.org/10.1007/s10453-013-9324-0

Herrero J., Polo, M.J., Moñino, A., Losada, MA. 2009. An energy balance snowmelt model in a Mediterranean site. J. Hydrol. 371, 98-107. https://doi.org/10.1016/j.jhydrol.2009.03.021

Hien, P. D., Loc, P. D., Dao, N. V. 2011. Air pollution episodes associated with East Asian winter monsoons. Sci. Total Environ., 409(23), 5063-5068. https://doi.org/10.1016/j.scitotenv.2011.08.049

Holloway, J., Neuman, J.A., Ryerson, T., Flocke, F., de Gouw, J., Atlas, E., Donnelly, S., Parrish, D. 2008. Lagrangian analysis of low altitude anthropogenic plume processing across the North Atlantic. Atmos. Chem. Phys. 8, 7737-7754. https://doi.org/10.5194/acp-8-7737-2008.

Houssos, E.E., Lolis, C.J., Bartzokas, A. 2007. The atmospheric conditions over Europe and the mediterranean, favoring snow events in Athens, Greece. Adv. Geosci. 12, 127-135. https://doi.org/10.5194/adgeo-12-127-2007

Izquierdo, R., Alarcón, M. and Àvila, A. 2013. WeMO effects on the amount and the chemistry of Winter precipitation in the north-eastern Iberian Peninsula. Tethys. 10, 45-51. http://dx.doi.org/10.3369/tethys.2013.10.05.

Jorba, O., Pérez, C., Rocadenbosch, F., Baldasano, J.M. 2004. Cluster Analysis of 4-Day Back Trajectories Arriving in the Barcelona Area, Spain, from 1997 to 2002. J. Appl. Meteorol. Climatol. 43(6), 887-901. https://doi.org/10.1175/1520-0450(2004)043<0887:CAODBT>2.0.CO;2.

Kaiser, A. 2009. Origin of polluted air masses in the Alps. An overview and first results for MONARPOP. Environ. Pollut. 157(12), 3232-3237. https://doi.org/10.1016/j.envpol.2009.05.042

Kaiser, A., Scheifinger, H., Spangl, W., Weiss, A., Gilge, S., Fricke, W., Ries, L., Cemas, D., Jesenovec, B. 2007. Transport of nitrogen oxides, carbon monoxide and ozone to the Alpine Global Atmosphere Watch stations Jungfraujoch (Switzerland), Zugspitze and Hohenpeissenberg (Germany), Sonnblick (Austria) and Mt. Krvavec (Slovenia). Atmos. Environ. 41, 9273-9287. https://doi.org/10.1016/j.atmosenv.2007.09.027.

Kassomenos, P., Vardoulakis, S., Borge, R. Lumbreras, C., Papaloukas, C., Karakitsios, S. 2010. Comparison of statistical clustering techniques for the classification of modelled atmospheric trajectories. Theor. Appl. Climatol. 102, 1-12. https://doi.org/10.1007/s00704-009-0233-7

Kassomenos, P., Vardoulakis, S., Borge, R., Lumbreras, J., Papaloukas, C., Karakitsios, S. 2010. Comparison of statistical clustering techniques for the classification of modelled atmospheric trajectories. Theor. Appl. Climatol. 102, 1-12. https://doi.org/10.1007/s00704-009-0233-7.

Kirk, J.P., Schmidlin, T.W. 2018. Moisture transport associated with large precipitation events inthe Upper Colorado River Basin. Int. J. Climatol. 38, 5323-5338. https://doi.org/10.1002/joc.5734

Kleshtanova, V., Tonchev, V., Stoycheva, A., Angelov, C. 2023. Cloud condensation nuclei and backward trajectories of air masses at Mt. Moussala in two months of 2016. J Atmos. Sol-Terr. Phy. 243, 106004. https://doi.org/10.1016/j.jastp.2023.106004.

Knippertz, P., Wernli, H. 2010. A lagrangian climatology of tropical moisture exports to the northern hemispheric extratropics. J. Clim. 23(4), 987-1003. https://doi.org/10.1175/2009JCLI3333.1.

Knippertz, P., Wernli, H., Gläser, G. 2013. A global climatology of tropical moisture exports. J. Clim. 26(10), 3031-3045. https://doi.org/10.1175/JCLI-D-12-00401.1

Knox, J. A., Rackley, J.A., Black, W., Gensini, V.A., Butler, M., Dunn, C., Gallo, T., Hunter, M.R., Lindsey, L., Phan, M., Scroggs, R., Brustad, S. 2013. Tornado debris characteristics and trajectories during the 27 April 2011 super outbreak as determined using social media data. B. Am. Meteorol. Soc. 94(9), 1371-1380. https://doi.org/10.1175/BAMS-D-12-00036.1.

Korgo, B., Roger, J.C., Bathiebo, J. 2013. Climatology of air mass trajectories and aerosol optical thickness over Ouagadougou. Global J. Pure Appl. Sci. 19, 169-181. http://dx.doi.org/10.4314/gjpas.v19i1.22

Kuhn, T., Damoah, R., Bacak, A., Sloan, J.J. 2010. Characterising aerosol trans-port into the Canadian High Arctic using aerosol mass spectrometry and Lagrangian modelling. Atmos. Chem. Phys. 10, 10489-10502. https://doi.org/10.5194/acp-10-10489-2010.

Levy, I., Dayan, U., Mahrer, Y. 2008. A five-year study of coastal recirculation and its effect on air pollutants over the East Mediterranean region. J. Geophys. Res. D: Atmos. 113(16), 16121. https://doi.org/10.1029/2007JD009529.

Li, M., Huang, X., Zhu, L., Li, J., Song, Y., Cai, X., Xie, S. 2012. Analysis of the transport pathways and potential sources of PM10 in Shanghai based on three methods. Sci. Total Environ. 414, 525-534, https://doi.org/10.1016/j.scitotenv.2011.10.054

Li, P., Li, X., Yang, C., Wang, X., Chen, J., Collett Jr. ,J.L. 2011. Fog water chemistry in Shanghai. Atmos. Environ. 45, 4034-4041.

Lozano, R.L., Hernández-Ceballos, M.A., San Miguel, E.G., Adame, J.A., Bolívar, J.P. 2012. Meteorological factors influencing the 7 Be and 210 Pb concentrations in surface airfrom the southwestern Iberian Peninsula. Atmos. Environ. 63,168-178. https://doi.org/10.1016/j.atmosenv.2012.09.052.

Martínez-Ibarra, E., Serrano-Montes, J.L., Arias-García, J. 2019. Reconstruction and analysis of 1900-2017 snowfall events on the southeast coast of Spain. Clim. Res. 78, 41-50. https://doi.org/10.3354/cr01557.

Mauger, G. S., Norris, J. R. 2010. Assessing the impact of meteorological history on subtropical cloud fraction. J. Clim. 23(11), 2926-2940. https://doi.org/10.1175/2010JCLI3272.1

Merino, A., Fernández, S., Hermida, L., López, L., Sánchez, J.L., García-Ortega, E., Gascón, E. 2014. Snowfall in the Northwest Iberian Peninsula: synoptic circulation patterns and their Influence on snow day trends. Sci. World J. 480275. https://doi.org/10.1155/2014/480275

Moltó, E. 2000. Grandes nevadas y percepción de las mismas en Alcoy. Investig Geográficas. 23, 102-118. https://doi.org/10.14198/INGEO2000.23.05.

Müller, G. V. Ambrizzi, T. 2010. Rossby wave propagation tracks in southern hemisphere mean basic flows associated to generalized frosts over southern South America. Atmósfera. 23(1), 25-35.

Notario, A., Adame, J.A., Bravo, I., Cuevas, C.A., Aranda, A., Díaz-de-Mera, Rodríguez, A. 2014. Air pollution in the plateau of the Iberian Peninsula. Atmos. Res. 145-146, 92-104. https://doi.org/10.1016/j.atmosres.2014.03.021.

Notaro, M., Alkolibi, F., Fadda, E., Bakhrjy, F. 2013. Trajectory analysis of Saudi Arabian dust storms. J. Geophys. Res.-Atmos. 118, 6028-6043. https://doi.10.1002/jgrd.50346.

Nuñez-Mora, J.A., Riesco Martín, J., Mora García, M. 2016. Climatological characteristics and synoptic patterns of snowfall episodes in the central Spanish Mediterranean area. Int. J. Climatol. 36, 4488-4496. https://doi.org/10.1002/joc.4645.

Obregón, M.A., Pereira, S., Wagner, F., Serrano, A., Cancillo, M.L., Silva, A.M. 2012. Regional differences of column aerosol parameters in western Iberian Peninsula. Atmos. Environ. 62, 208-219. http://dx.doi.org/10.1016/j.atmosenv.2012.08.016.

Olcina, J., Moltó, E. 1999. La nevada de 1926: Repercusiones en la montaña alcoyana (Alicante). Nimbus. Rev. Climat., Meteorol. Paisaje. 3, 105-138.

Ortega, Mª.T., Morales, C.G. 2023. Methodology for the historical and synoptic analysis of snows: its application to the region of Castilla y León (Spain). Theor. Appl. Climatol. 151,1825-1853. https://doi.org/10.1007/s00704-022-04336-6.

Ortiz-Amezcua, P., Guerrero-Rascado, J. L., Granados-Muñoz, M. J., Bravo-Aranda, J. A., Alados-Arboledas, L. 2014. Characterization of atmospheric aerosols for a long range transport of biomass burning particles from Canadian forest fires over the southern Iberian Peninsula in July 2013. Opt. Pura Apl. 47(1): 43-49. https://doi.org/10.7149/OPA.47.1.43.

Osada, K., Kido, M., Iida, H., Matsunaga, K., Iwasaka, Y., Nagatani, M., Nakada, H. 2003. Seasonal variation of free tropospheric aerosol particles at Mt. Tateyama, central Japan. J. Geophys. Res. D: Atmos. 108(23), 8667. https://doi.org/10.1029/2003JD003544.

Pérez, I. A., Sánchez, M. L., García, A., Pardo, N. 2012. Spatial analysis of CO2 concentration in an unpolluted environment in northern Spain. J Environ Manage. 113, 417-425. https://doi.org/10.1016/j.jenvman.2012.09.023.

Pérez, I. A., Sánchez, M. L., García, A., Pardo, N. 2018a. Influence of air parcel trajectories on CO2 and CH4 concentrations in the northern plateau of the Iberian Peninsula. J Atmos Sol-Terr Phy. 167, 58-65. https://doi.org/10.1016/j.jastp.2017.10.015.

Pérez, I.A., Sánchez, M. L., García, M. Á., Pardo, N. and Fernández-Duque, B. 2018b. Analysis of the airflow at the centre of the upper plateau on the Iberian Peninsula and its link to CO2 and CH4 concentrations. Int. J. Climatol. 38, 2126-2137. https://doi.org/10.1002/joc.5323.

Pérez, I.A., Artuso, F., Mahmud, M., Kulshrestha, U., Sánchez, M.L., García, M. Á. 2015. Applications of Air Trajectories. Adv. Meteorol. 284213 https://doi.org/10.1155/2015/284213.

Pérez, I.A., Luisa Sánchez, M., García, M.Á., Pardo, N. 2019. Sensitivity of CO2 and CH4 Annual Cycles to Different Meteorological Variables at a Rural Site in Northern Spain. Adv. Meteorol. 9240568. https://doi.org/10.1155/2019/9240568.

Pérez-Palazón, M.J., Rafael-Pimentel, R., Polo, M.J. 2018: Climate trends impact on the snowfall regime in Mediterranean mountain areas: future scenario assessment in Sierra Nevada (Spain). Water. 10(6), 720. https://doi.org/10.3390/w10060720.

Perry, L. B., Konrad, C. E., Schmidlin, T. W. 2007. Antecedent upstream air trajectories associated with northwest flow snowfall in the Southern Appalachians. Weather Forecast. 22(2) pp. 334-352. https://doi.org/10.1175/WAF978.1.

Pfahl, S., Niedermann, N. 2011. Daily covariations in near-surface relative humidity and temperature over the ocean. J. Geophys. Res. D: Atmos. 116(19), D19104. https://doi.org/10.1029/2011JD015792.

Pollina, J. B., Colle, B. A., Charney, J. J. 2013. Climatology and meteorological evolution of major wildfire events over the Northeast United States. Weather Forecast. 28(1), 175-193. ttps://doi.org/10.1175/WAF-D-12-00009.1.

Pons, M.R., San-Martín, D., Herrera, S., Gutiérrez, J.M. 2010. Snow trends in Northern Spain: analysis and simulation with statistical downscaling methods. Int. J. Climatol. 30, 1795-1806. https://doi.org/10.1002/joc.2016

Räty, M., Sogacheva, L., Keskinen, H.-M., Kerminen, V.-M., Nieminen, T., Petäjä, T., Ezhova, E., Kulmala, M. 2023. Dynamics of aerosol, humidity, and clouds in air masses travelling over Fennoscandian boreal forests. Atmos. Chem. Phys. 23, 3779-3798. https://doi.org/10.5194/acp-23-3779-2023.

Real, E., Law, K.S., Schlager, H., Roiger, A., Huntrieser, H., Methven, J., Cain, M.,

Revuelta, M.A., Sastre, M., Fernández, A.J., Martín, L., García, R., Gómez-Moreno, F.J., Artíñano, B., Pujadas, M., Molero, F. 2012. Characterization of the Eyjafjallajökull volcanic plume over the Iberian Peninsula by lidar remote sensing and ground-level data collection. Atmos. Environ. 48, 46-55. https://doi.org/10.1016/j.atmosenv.2011.05.033.

Roberge, A., Gyakum, J. R., Atallah, E.H. 2009. Analysis of intense poleward water vapor transports into high latitudes ofWestern North America. Weather Forecast. 24(6), 1732-1747. https://doi.org/10.1175/2009WAF2222198.1.

Ruíz, E. (dir.) 1998. El clima del País Vasco a través de la prensa. Euskal Herriko Klima prentsaren bidez, Servicio Vasco de Meteorologia del Gobierno Vasco, Vitoria.

Saavedra, S., Rodríguez, A., Taboada, J.J., Souto, J.A., Casares, J.J. 2012. Synoptic patterns and air mass transport during ozone episodes in northwestern Iberia. Sci. Total Environ. 441, 97-110. https://doi.org/10.1016/j.scitotenv.2012.09.014.

Salamanca-Salamanca, M. 2012. Aproximació a l´innivació a Mallorca en època contemporània (MS thesis). Universitat de les Illes Balears, Palma de Mallorca. http://ibdigital.uib.es/greenstone/sites/localsite/collect/memoriesUIB/index/assoc/Salamanc.dir/Salamanca_Salamanca_Miquel.pdf (accessed 10 April 2023)

Salamanca-Salamanca, M., Tomas-Burguera, M., Grimalt, M. 2012. Climatología de las irrupciones de aire frío en Mallorca durante el periodo 1980–2010 a partir de la temperatura a 850 hPa. Intensidad, distribución, temporal, tipos de tiempo asociados y su correlación con los días de nieve, in: Rodríguez-Puebla, C., Ceballos-Salvador, A., González-Reviriego, N., Morán-Tejeda, E., Hernández-Encinas, A. (Eds.), Cambio climático. Extremos e impactos. Asociación Española de Climatología, Madrid, pp. 623-630.

Artinano, B., Pio, C., Afonso, J., Legrand, M., Puxbaum, H., Hammer, S., 2010. Evaluation of aerosol sources at European high altitude background sites with trajectory statistical methods. Atmos. Environ., 44, 2316-2329. https://doi.org/10.1016/j.atmosenv.2010.03.042.

San José, R., Stohl, A., Karatzas, K., Bohler, T., James, P., Pérez, J.L. 2005. A modelling study of an extraordinary night time ozone episode over Madrid domain. Environ. Model. Softw. 20, 587-593. https://doi.org/10.1016/j.envsoft.2004.03.009.

Santos, P.S.M., Santos, E.B.H., Duarte, A.C. 2013. Seasonal and air mass trajectory effects on dissolved organic matter of bulk deposition at a coastal town in south-western Europe. Environ. Sci. Pollut. 20, 227-237. https://doi.org/10.1007/s11356-012-0971-4.

Satyawali, P.K., Schneebeli, M., Pielmeier, C., Stucki, T., Singh, A.K. 2009. Preliminary characterization of Alpine snow using SnowMicroPen. Cold Reg. Sci. Technol. 55, 311-320. https://doi.org/10.1016/j.coldregions.2008.09.003

Schelfinger, H., Kaiser, A. 2007. Validation of trajectory statistical methods. Atmos. Environ. 41, 8846-8856. https://doi.org/10.1016/j.atmosenv.2007.08.034.

Scherrer, S.C., Wüthrich, C., Croci-Maspoli, M., Weingartner, R., Appenzeller, C. 2013. Snow variability in the Swiss Alps 1864–2009. Int. J. Climatol. 33, 3162-3173. https://doi: 10.1002/joc.3653.

Seagram, A., Steyn, D., Ainslie, B. 2014. Modelled recirculation of pollutants during ozone episodes in the Lower Fraser Valley, in: Steyn, D., Builtjes, P., Timmermans, R. (Eds.), Air Pollution Modeling and its Application XXII. Springer, Dordrecht, pp. 291-295.

Shi, C., Yang, J., Qiu, M., Zhang, H., Zhang, S., Li, Z. 2010. Analysis of an extremely dense regional fog event in Eastern China using a mesoscale model. Atmos. Res. 95(4), 428-440. https://doi.org/10.1016/j.atmosres.2009.11.006.

Solberg, S., Hov, O., Sovde, A., Isaksen, I.S.A., Coddeville, P., De Backer, H., Forster, C., Orsolini, Y., Uhse, K. 2008. European surface ozone in the extreme summer 2003. J. Geophys. Res. Atmos. 113, D07307. https://doi.org/10.1029/2007JD009098.

Soltani, M., Babu, C. A., Mofidi, A. 2014. Meteorological aspects of an abnormal cooling event over Iran in April 2009. Meteor. Atmos. Phys. 124(1-2), 47-65. https://doi.org/10.1007/s00703-014-0309-5.

Soncini, A., Bocchiola, D. 2011. Assessment of future snowfall regimes within the Italian Alps using general circulation models. Cold Reg Sci Technol. 68, 113-123. https://doi.org/10.1016/j.coldregions.2011.06.011.

Stein, A.F., Wang, Y., de la Rosa, J. D., Sánchez de la Campa, A. M., Castell, N., Draxlet, R. R. 2011. Modeling PM10 Originating from Dust Intrusions in the Southern Iberian Peninsula Using HYSPLIT. Weather Forecast. 26(2), 236-242. https://doi.org/10.1175/WAF-D-10-05044.1.

Steinhauser, F. (dir.) 1970. Atlas climático de Europa. UNESCO, Geneva.

Stohl, A. 1999. The FLEXTRA trajectory model version 3.0, user´s guide. University of Munich, Munich.

Stohl, A., 1996. Trajectory statistics -a new method to establish source- receptor relationships of air pollutants and its application to the transport of particulate sulfate in Europe. Atmos. Environ. 30, 579-587. https://doi.org/10.1016/1352-2310(95)00314-2.

Stohl, A., Seibert, P. 1998. Accuracy of trajectories as determined from the conservation of meteorological tracers. Q.J.R. Meteorol. Soc. 124, 1465-1484. https://doi.org/10.1002/qj.49712454907.

Stohl, A., Wotawa, G., Seibert, P., Krompkolb, H. 1995. Interpolation errors in wind fields as a function of spatial and temporal resoloution and their impact on different types of kinematic trajectories. J. Appl. Meteorol. 34, 2149-2165. https://doi.org/10.1175/1520-0450(1995)034<2149:IEIWFA>2.0.CO;2.

Szwed, M., Pinskwar, I., Kundzewicz, Z.W., Graczyk, D. and Mezghani, A. 2017. Changes of snow cover in Poland. Acta Geophys. 65, 65-76. https://doi.org/10.1007/s11600-017-0007-z.

Toledano, C., Cachorro, V.E., De Frutos, A.M., Torres, B., Berjón, A., Sorribas, M., Stone, R.S. 2009. Airmass classification and analysis of aerosol types at El Arenosillo (Spain). J. Appl. Meteorol. Climatol. 48, 962-981. https://doi.org/10.1175/2008JAMC2006.1.

Tomás-Quevedo, A. (1976). La nieve en la ciudad condal. Miscellanea Barcinonensia. 45, 45-57.

Tosic, I., Unkasevic, M. 2013. Extreme daily precipitation in Belgrade and their links with the prevailing directions of the air trajectories. Theor. Appl. Climatol. 111(1-2), 97-107. https://doi.org/10.1007/s00704-012-0647-5

Trapero, L., Bech, J., Duffourg, F., Esteban, P., Lorente, J. 2013. Mesoscale numerical analysis of the historical November 1982 heavy precipitation event over Andorra (Eastern

Pyrenees). Nat. Hazards Earth Syst. Sci. 13(11), 2969-2990. https://doi.org/10.5194/nhess-13-2969-2013.

Traub, M., Fischer, H., de Reus, M., Kormann, R., Heland, J., Ziereis, H., Schlager, H., Holzinger, R., Williams, J., Warneke, C., de Gouw, J., Lelieveld, J. 2003. Chemical characteristics assigned to trajectory clusters during the MINOS campaign. Atmos. Chem. Phys. 3, 459-468. https://doi.org/10.5194/acp-3-459-2003.

Valenzuela, A., Olmo, F. J., Lyamani, H., Antón, M. Quirantes, A., and Alados-Arboledas, L. 2012. Classification of aerosol radiative properties during African desert dust intrusions over southeastern Spain by sector origins and cluster analysis. J. Geophys. Res. 117, D06214. https://doi.org/10.1029/2011JD016885.

Valt, M., Cagnati, A., Crepaz, A. Cat Berro, D. 2008. Variazioni recenti del manto nevoso sul versante meridionale delle Alpi. Neve e Valanghe. 63, 46-57.

Vicente-Serrano, S.M., Rodríguez-Camino, E., Domínguez-Castro, F., El Kenawy, A., Azorín-Molina, C. 2017. An updated review on recent trends in observational surface atmospheric variables and their extremes over Spain. Cuad. Invest. Geogr. 43, 209-232. https://doi.org/10.18172/cig.3134.

Walna, B., Kurzyca, I., Bednorz, E., Kolendowicz, L. 2013. Fluoride pollution of atmospheric precipitation and its relationship with air circulation and weather patterns (Wielkopolski National Park, Poland). Environ. Monit. Assess. 185(7), 5497-5514. https://doi.org/10.1007/s10661-012-2962-9.

Westgate, J. N., Sofowote, U. M., Roach, P., Fellin, P., D'Sa, I., Sverko, E., Su, Y., Hung, Y., Wania, F. 2013. In search of potential source regions of semi-volatile organic contaminants in air in the Yukon Territory, Canada from 2007 to using hybrid receptor models. Environ. Chem. 10(1), 22-33. https://doi.org/10.1071/EN12164

Wilson, J. W., Knight, C. A., Tessendorf, S. A., Weeks, C. 2011. Polarimetric radar analysis of raindrop size variability in maritime and continental clouds. J. Appl. Meteorol. Climatol. 50(9), 1970-1980. https://doi.org/10.1175/2011JAMC2683.1.

Yan, G., Kim, G. 2012. Dissolved organic carbón in the precipitation of Seoul, Korea: Implications for global wet depositional flux of fossil-fuel derived organic carbon. Atmos. Environ. 59,117-124.https://doi.org/10.1016/j.atmosenv.2012.05.044.

Zeng, J., Matsunaga, T., Mukai, H. 2010. METEX-a flexible tool for air trajectory calculation. Environ. Model. Softw. 25(4), 607-608. https://doi.org/10.1016/j.envsoft.2008.10.015.

Zhangqun Li, Z., Xiao, Z. 2020. Analyze on the contribution of the moisture sources to the precipitation over mid-low Lancang River nearby región and its variability in the beginning of wet season. Theor. Appl. Climatol. 141, 775-789. https://doi.org/10.1007/s00704-020-03228-x.